JOURNAL OF VIROLOGY, June 2010, p. 5615–5626 Vol. 84, No. 11
0022-538X/10/$12.00 doi:10.1128/JVI.02094-09

Bocavirus Infection Induces Mitochondrion-Mediated Apoptosis and Cell Cycle Arrest at G_2/M Phase[▽]

Aaron Yun Chen, Yong Luo, Fang Cheng, Yuning Sun,† and Jianming Qiu*

Department of Microbiology, Molecular Genetics and Immunology, University of Kansas Medical Center, Kansas City, Kansas 66160

Received 2 October 2009/Accepted 8 March 2010

Bocavirus **is a newly classified genus of the family** ***Parvovirinae*****. Infection with** ***Bocavirus*** **minute virus of canines (MVC) produces a strong cytopathic effect in permissive Walter Reed/3873D (WRD) canine cells. We have systematically characterized the MVC infection-produced cytopathic effect in WRD cells, namely, the cell death and cell cycle arrest, and carefully examined how MVC infection induces the cytopathic effect. We found that MVC infection induces an apoptotic cell death characterized by Bax translocalization to the mitochondrial outer membrane, disruption of the mitochondrial outer membrane potential, and caspase activation. Moreover, we observed that the activation of caspases occurred only when the MVC genome was replicating, suggesting that replication of the MVC genome induces apoptosis. MVC infection also induced a gradual cell cycle arrest from the S phase in early infection to the G_2/M phase at a later stage, which was confirmed by the upregulation of cyclin B1 and phosphorylation of cdc2. Cell cycle arrest at the G_2/M phase was reproduced by transfection of a nonreplicative NS1 knockout mutant of the MVC infectious clone, as well as by inoculation of UV-irradiated MVC. In contrast with other parvoviruses, only expression of the MVC proteins by transfection did not induce apoptosis or cell cycle arrest. Taken together, our results demonstrate that MVC infection induces a mitochondrion-mediated apoptosis that is dependent on the replication of the viral genome, and the MVC genome** ***per se*** **is able to arrest the cell cycle at the G_2/M phase. Our results may shed light on the molecular pathogenesis of** ***Bocavirus*** **infection in general.**

The *Bocavirus* genus is newly classified within the subfamily *Parvovirinae* of the family *Parvoviridae* (21). The currently known members of the *Bocavirus* genus include bovine parvovirus type 1 (BPV1) (17), minute virus of canines (MVC) (57), and the recently identified human bocaviruses (HBoV, HBoV2, and HBoV3) (4, 7, 36).

MVC was first recovered from canine fecal samples in 1970 (10). The virus causes respiratory disease with breathing difficulty (14, 32, 49) and enteritis with severe diarrhea (11, 39), which often occurs with coinfection with other viruses (39), spontaneous abortion of fetuses, and death of newborn puppies (14, 29). Pathological lesions in fetuses in experimental infections were found in the lymphoid tissue of the lung and small intestine (14). MVC was isolated and grown in the Walter Reed/3873D (WRD) canine cell line (10), which is derived from a subdermoid cyst of an irradiated male dog (10). The full-length 5.4-kb genome of MVC was recently mapped with palindromic termini (60). Under the control of a single P6 promoter, through the mechanism of alternative splicing and alternative polyadenylation, MVC expresses two nonstructural proteins (NS1 and NP1) and two capsid proteins (VP1 and VP2). Like the NS1 proteins of other parvoviruses, the NS1 of MVC is indispensable for genome replication. The NP1 protein, which is unique to the *Bocavirus* genus, appears to be critical for optimal viral replication, as the NP1 knockout mutant of MVC suffers from severe impairment of replication (60). A severe cytopathic effect during MVC infection of WRD cells has been documented (10, 60).

The HBoV genome has been frequently detected worldwide in respiratory specimens from children under 2 years old with acute respiratory illnesses (2, 34, 55). HBoV is associated with acute expiratory wheezing and pneumonia (3, 34, 55) and is commonly detected in association with other respiratory viruses (34, 55). Further studies are necessary, however, to identify potential associations of HBoV infection with clinical symptoms or disease of acute gastroenteritis (7, 36). The full-length sequence of infectious MVC DNA (GenBank accession no. FJ214110) that we have reported shows 52.6% identity to HBoV, while the NS1, NP1, and VP1 proteins are 38.5%, 39.9%, and 43.7% identical to those of HBoV, respectively (60).

The cytopathic effect induced during parvovirus infection has been widely documented, e.g., in infections with minute virus of mice (MVM) (13), human parvovirus B19 (B19V) (58), parvovirus H-1 (25, 52), and BPV1 (1). In *Bocavirus*, cell death during BPV1 infection of embryonic bovine tracheal cells has been shown to be achieved through necrosis, independent of apoptosis (1). B19V-induced cell death of primary erythroid progenitor cells has been shown to be mainly mediated by an apoptotic pathway (58) in which the nonstructural protein 11kDa plays a key role (16). In contrast, the MVM-induced cytopathic effect has been revealed to be mediated by NS1 interference with intracellular casein kinase II (CKII) signaling (22, 44, 45), a nonapoptotic cell death. Oncolytic parvovirus H-1 infections can induce either apoptosis or nonapoptotic cell death, depending on the cell type (25, 40). Therefore, the mechanisms underlying parvovirus infection-induced cell death vary, although NS1 has been widely shown

* Corresponding author. Mailing address: Department of Microbiology, Molecular Genetics and Immunology, University of Kansas Medical Center, Mail Stop 3029, 3901 Rainbow Blvd., Kansas City, KS 66160. Phone: (913) 588-4329. Fax: (913) 588-7295. E-mail: jqiu@kumc.edu.

† Present address: Department of Biochemistry and Molecular Biology, Ningxia Medical University, Key Lab of Reproduction and Heredity of Ningxia Hui Autonomous Region, Yinchuan, Ningxia 750004, China.

▽ Published ahead of print on 24 March 2010.

to be involved in both apoptotic and nonapoptotic cell death. The nature of the cytopathic effect during *Bocavirus* MVC infection has not been studied.

Parvovirus replication requires infected cells at the S phase. Infection with parvovirus has been revealed to accompany a cell cycle perturbation that mostly leads to an arrest in the S/G_2 phase or the G_2/M phase during infection (30, 33, 42, 47, 65). MVM NS1 expression induces an accumulation of sensitive cells in the S/G_2 phase (6, 46, 47). Whether MVC infection-induced cell death is accompanied by an alternation of cell cycle progression and whether the viral nonstructural protein is involved in these processes have not been addressed.

In this study, we found, in contrast with other members of the family *Parvoviridae*, expression of both the nonstructural and structural proteins of MVC by transfection did not induce cell death or cell cycle arrest. However, the cytopathic effect induced during MVC infection is a replication-coupled, mitochondrion-mediated and caspase-dependent apoptosis, accompanied with a gradual cell cycle arrest from the S phase to the G_2/M phase, which is facilitated by the MVC genome.

MATERIALS AND METHODS

Cells and virus. WRD cells (10) were maintained in Dulbecco's modified Eagle's medium with 10% fetal calf serum in 5% CO_2 at 37°C. The MVC used in this study, the original strain GA3, was isolated at the School of Veterinary Science, Cornell University. MVC was cultured and quantified as previously described (60), and the virus titer was determined as the number of fluorescence focus-forming units (FFU) per ml (12). The WRD cell line and MVC were obtained as gifts from C. Parrish (Cornell University).

MVC was inactivated by UV irradiation as follows. To each well of a 96-well plate, 50 μl of purified MVC (60) containing the cell culture medium was added. The plate was placed in a Hoefer UVC 500 UV cross-linker (Hoefer, Inc.) for UV irradiation at a dose of 720 mJ/cm^2 (26, 38).

Infection and transfection. WRD cells were seeded 1 day prior to infection or transfection. MVC at the indicated multiplicity of infection (MOI; FFU/cell) was added to the culture right after the medium was refreshed.

Transfection was performed using the LipoD293 transfection reagent (SignaGen Laboratories, MD) following the manufacturer's instructions.

Plasmid constructs. All of the nucleotide numbers of MVC refer to the MVC GA3 isolate (GenBank accession no. FJ214110).

(i) Constructs for expressing nonstructural proteins. The NS1 open reading frames (ORFs) (nucleotides [nt] 403 to 2724), NP1 ORF (nt 2537 to 3094), and VP1 ORF (nt 3081 to 5192) were inserted separately into BamHI/XhoI-digested pcDNAGFP vector (19) to construct the pGFP-NS1, pGFP-NP1, and pGFP-VP1, respectively. pMVCNSCap was constructed by inserting the MVC sequence of nt 150 to 5305 into SacII-ApaI-digested pBluescript SK(+) (Stratagene).

(ii) Mutants of infectious clone pIMVC. The MVC infectious clone, pIMVC, and its derivatives pIMVCNS1(−), pIMVCNP1(−), pIMVCVP1(−), and pIMVCVP2(−) were described previously (60). pIMVCVP1/2(−) was constructed by combing the VP1 and VP2 ATG mutations in pIMVC. pIMVCΔ1/2LTR was constructed by deleting the MVC sequences of nt 1 to 101 in the left palindromic repeat of the pIMVC through NotI digestion.

(iii) Construct for GST-fusion expression. For glutathione *S*-transferase (GST)-fusion expression, the MVC NP1 ORF (nt 2537 to 3094) was cloned into pGEX4T3 (GE Health) as pGEX-MVCNP1.

Antibodies. GST-fused MVC NP1 protein was expressed from pGEX-MVCNP1-transformed *Escherichia coli* BL21 cells and purified as described previously (60). The anti-NP1 antiserum was produced by immunizing animals with purified GST-MVCNP1 following a protocol described previously (60). The animal protocol used was approved by the University of Kansas Medical Center Institutional Animal Care and Use Committee.

Anti-Bax, anti-cyclin B1, anti-phospho-cdc2 (pY15), and anti-cyclin A were purchased from BD Biosciences. Anti-β-actin (clone AC-15) was purchased from Sigma. We used dilutions of antibodies for Western blotting and immunofluorescence as suggested in the manufacturers' instructions.

SDS-PAGE, Western blotting, and immunofluorescence. SDS-PAGE, Western blotting, and the immunofluorescence assay were performed as previously described (27, 50, 60). Mitochondria were stained by incubating cells with a mitochondrion-staining specific dye, MitoTracker Red CMXRos (Invitrogen), at 500 nM in the cell culture medium for 30 min before fixation in ice-cold acetone. Confocal images were taken at a magnification of 60× (objective lens) with an Eclipse C1 Plus confocal microscope (Nikon) controlled by Nikon EZ-C1 software.

Southern blotting. WRD cells were transfected with the MVC constructs as shown in Fig. 3C. At 48 h posttransfection, low-molecular-weight DNA (Hirt DNA) was extracted from transfected cells as described previously (27). Southern blotting was performed as described previously (48) using the MVC NSCap probe (60).

Flow cytometry analysis. (i) Annexin V-PI staining. Cells were dissociated by 0.25% trypsin in EDTA buffer. The cells were recovered in culture medium at 37°C for 30 min with agitation prior to staining and then washed twice with annexin V binding buffer. Of these cells, 1×10^6 were resuspended in 100 μl of annexin V binding buffer, followed by the addition of 5 μl Cy5-conjugated annexin V (BD Biosciences) and 5 μl propidium iodide (PI) (60 μg/ml, Sigma). The mixture was then incubated at room temperature (RT) for 15 min, followed by the addition of 400 μl annexin V binding buffer. Flow cytometry was performed after staining.

FLICA assay and FLICA-Live/Dead Violet costaining. Cells were dissociated by 0.25% trypsin in EDTA and stained with carboxyfluorescein (FAM)-labeled FLICA (fluorochrome-labeled inhibitor of caspase) peptides (Immunochemistry Tech, MN), FAM-VAD-FMK (poly-FLICA), FAM-DEVD-FMK (caspase 3 and 7 FLICA), FAM-VEID-FMK (caspase 6 FLICA), FAM-LETD-FMK (caspase 8 FLICA), FAM-LEHD-FMK (caspase 9 FLICA), FAM-AEVD-FMK (caspase 10 FLICA), and the fluorescein isothiocyanate (FITC)-labeled FLICA peptide (Biovision), FITC-ATAD-FMK (caspase 12 FLICA), as described previously (20).

For FLICA-Live/Dead Violet costaining, cells were stained with FAM-VAD-FMK (poly-FLICA peptide) followed by Live/Dead Violet staining (Invitrogen) according to the manufacturer's instructions. Specifically, 2 μl of poly-FLICA reagent was added to 300 μl of cell suspension (10^6 cells/ml in phosphate-buffered saline PBS containing 2% fetal calf serum [FCS]), which was incubated at 37°C for 1 h. The cells were washed once with PBS–2% FCS and resuspended in 500 μl of PBS–2% FCS with 1 μl of Live/Dead Violet dye. The mixture was kept on ice for 30 min. Cells were then washed twice with PBS–2% FCS and fixed in 1% paraformaldehyde for 30 min before analysis. For costaining with anti-NS1 of MVC, fixed cells were permeabilized in PBS–2% FCS containing 0.2% Tween 20 (PBST) for 30 min and stained with a 1:50 dilution of anti-NS1 antiserum, followed by staining with a Cy5-labeled secondary antibody.

DAPI staining. Cells were dissociated by 0.25% trypsin in EDTA and fixed in 1% paraformaldehyde at RT for 30 min. The cells were washed, stained with DAPI (4′,6-diamidino-2-phenylindole), at 20 μg/ml in PBST, and then analyzed by flow cytometry. When costaining was required, cells were first stained with anti-NS1 or anti-NP1 followed by DAPI staining.

Cell proliferation assay (DDAO staining). DDAO [7-hydroxy-9H-(1,3-dichloro-9,9-dimethylacridin-2-one)], a fixable, far-red-fluorescent tracer for very-long-term cell labeling, was purchased from Invitrogen and applied following the manufacturer's instructions. Briefly, every 5 million cells were collected and washed twice with prewarmed PBS. The cells were then resuspended in 1 ml of 10 μM DDAO in PBS and kept at 37°C for 10 min. The mixture was then immediately transferred to 15 ml of prewarmed cell culture medium to quench the reaction. After cells were washed twice with the warmed medium, they were then resuspended in the medium and incubated at 37°C. The next day, stained cells were used for either MVC infection or transfection. When required, DDAO-stained cells were fixed and further stained intracellularly with anti-NS1. DDAO fluorescence decays when cells proliferate; therefore, the lower the fluorescence detected, the better the proliferation of cells (see Fig. 1D and 4D).

MOMP detection [DiIC$_1$(5)-PI or -poly-FLICA costaining]. The level of mitochondrial outer membrane permeabilization (MOMP) was determined with the MitoProbe DiIC$_1$(5) assay kit (Invitrogen). DiIC$_1$(5) (1′,1′,3,3,3′,3′-hexamethylindodicarbo-cyanine iodide) accumulates primarily in mitochondria with active mitochondrial membrane potentials. DiIC$_1$(5) staining decreases as the mitochondrial membrane potential is reduced. Cell membrane permeability was probed by propidium iodide (PI; Sigma). Costaining of DiIC$_1$(5) with PI was performed following the manufacturer's instruction (Invitrogen). Briefly, WRD cells were trypsinized and resuspended at 10^6 cells/ml of the cell culture medium, into which 5 μl of DiIC$_1$(5) at 10 μM in dimethyl sulfoxide (DMSO) was added, followed by incubation at 37°C for 15 min. PI was added to the mixture to a final concentration of 0.3 μg/ml. The mixture was then incubated for another 15 min at 37°C. For costaining with poly-FLICA peptide, cells were stained with poly-FLICA for 30 min at 37°C prior to the addition of DiIC$_1$(5) and then incubated

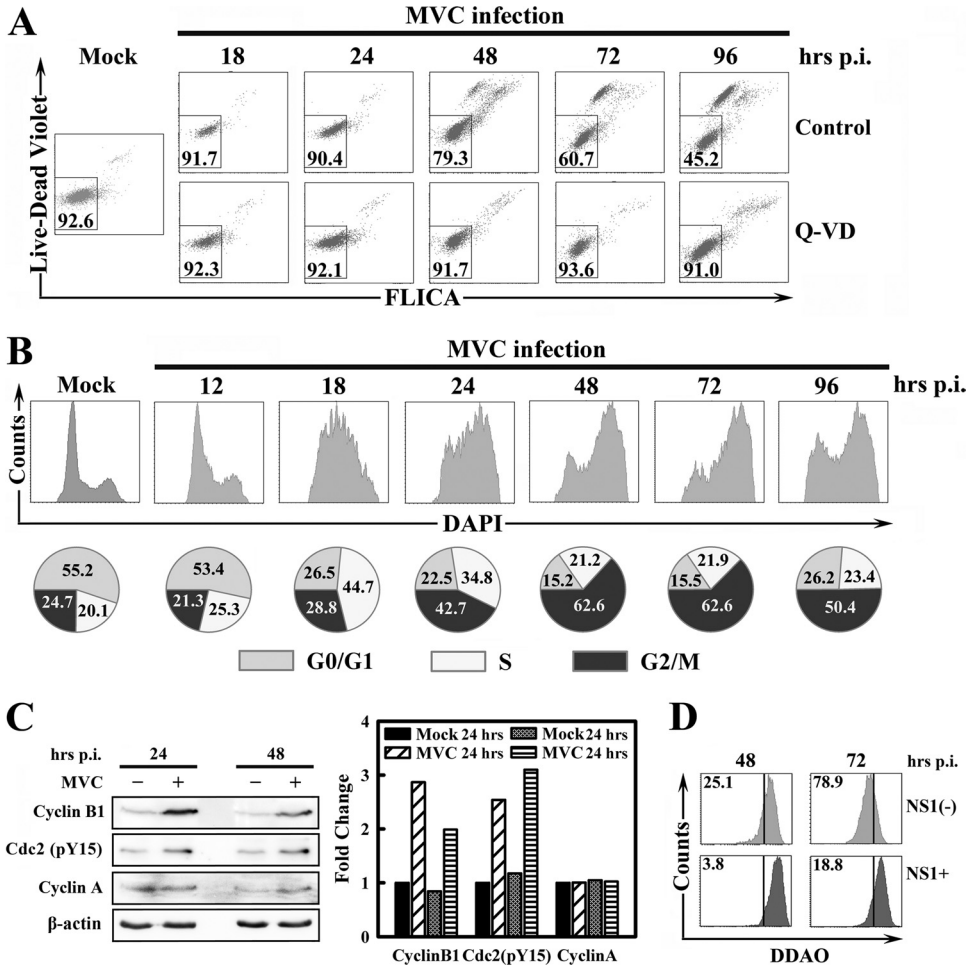

FIG. 1. MVC infection induces apoptosis and cell cycle arrest. WRD cells were infected with MVC at an MOI of 3. (A) Cells were cultured in media supplemented with DMSO as a control or a pan-caspase inhibitor Q-VD (R&D Systems) at 40 μM immediately after infection. At indicated times p.i., infected cells were triple stained by anti-NS1, Live/Dead Violet, and poly-FLICA. Anti-NS1-stained cells were selected and plotted as Live/Dead Violet versus poly-FLICA fluorescence. The percentage of live cells (double negative) is shown in the square gate. (B) At the indicated times p.i., cells were double stained by anti-NS1 and DAPI. The anti-NS1-stained cells were selected and plotted as cell counts versus DAPI staining. Percentages of cells in the G_0/G_1, S, and G_2/M phases are shown in circle graphs at the bottom of the panel. (C) Mock- and MVC-infected WRD cells were harvested at 24 h and 48 h p.i., respectively. Cell lysates were subjected to Western blotting using anti-cyclin B1, anti-cdc2 (pY15), anti-cyclin A, and anti-β-actin, respectively. The levels of signals on blots, which are normalized to the level of β-actin, are shown in the bar chart to the right. The normalized value of the mock cells at 24 h is arbitrarily set to 1. (D) At 24 h and 48 h p.i., MVC-infected WRD cells were stained with DDAO and anti-NS1. Both anti-NS1-positive (NS1+) and anti-NS1-negative [NS1(−)] populations were gated and plotted as histograms of cell counts versus DDAO signal. Numbers as shown are percentages of proliferated cells. The line as shown is arbitrarily set based on the nonproliferated control cells, which were fixed immediately after infection. A representative of two independent experiments is shown in panels A to D.

at 37°C for another 30 min. CCCP (carbonyl cyanide 3-chlorophenylhydrazone) was used as a positive control for disruption of mitochondrial outer membrane potential at a final concentration of 50 μM. The stained cells were analyzed on a flow cytometer.

All of the samples were analyzed on a three-laser flow cytometer (LSR II; BD Biosciences) within an hour of staining at the Flow Cytometry Core of the University of Kansas Medical Center. All flow cytometry data were analyzed using FACS DIVA software (BD Biosciences).

RESULTS

MVC infection induces cell death and cell cycle arrest in WRD cells. To analyze cell death and cell cycle arrest induced during MVC infection, we infected WRD cells with MVC and stained them with anti-NS1, Live/Dead Violet, and FAM-VAD-FMK (poly-FLICA peptide) at the indicated times postinfection (p.i.). We selected the MVC-infected cells, which were anti-NS1 positive, and plotted as Live/Dead Violet fluorescence versus FLICA fluorescence intensity in Fig. 1A. MVC infection induced a cell death in a time-dependent manner during infection, as shown by the Live/Dead Violet staining. From 18 to 96 h p.i., the live cell population (Live/Dead$^-$) decreased from 91.7% to 45.2% (Fig. 1A; control). In addition, dead cells (Live/Dead$^+$) in the control group were almost all stained with FAM-VAD-FMK (poly-FLICA$^+$), indicating that caspases were activated in all the dead cells (Fig. 1A; control). Active caspase is a hallmark of apoptotic cell death (24). This result indicates that MVC infection induces an apoptotic cell

death. Moreover, with the addition of a specific pan-caspase inhibitor, Q-VD-OPH (Q-VD), cell death in MVC-infected cells was inhibited even at 96 h p.i. (Fig. 1A; Q-VD). Q-VD is a newly developed pan-caspase inhibitor without significant cross-reactivity with cathepsin (15). Thus, the rescue of cell death by Q-VD further confirmed the apoptotic nature of MVC infection-induced cell death.

MVC infection not only induced apoptosis but also induced a severe cell cycle arrest of infected WRD cells. We gated MVC NS1-expressing cells and plotted them in the histogram of DAPI staining (Fig. 1B). Cell cycle analysis of MVC-infected cells by DAPI staining showed a clear transition from an S-phase accumulation to a G_2/M arrest during MVC infection (Fig. 1B). As early as 18 h p.i., we observed a widened peak with apex in the S phase (Fig. 1B; 18 h p.i.). Only 6 h later, the S-phase accumulation became weaker and was replaced by G_2/M arrest at 24 h p.i. (Fig. 1B; 24 h p.i.). After that, the cell cycle of NS1-expressing cells was mostly seized in the G_2/M phase (Fig. 1B, 48, 72, and 96 h p.i., respectively). The Q-VD treatment, while completely abolishing the apoptosis induced by MVC infection (Fig. 1A; Q-VD), did not change the cell cycle perturbation (data not shown). To further support the observation that MVC infection induced cell cycle arrest, we used Western blotting to probe the level of cell cycle regulatory proteins, cyclin B1, phospho-cdc2 (pY15), and cyclin A. As shown in Fig. 1C, G_2/M-phase checkpoint regulators cyclin B1 and phospho-cdc2 (pY15) were both upregulated at 24 and 48 h p.i. in MVC-infected cells. Cyclin A, which is required for S-phase passage, did not differ significantly between mock- and MVC-infected cell groups.

We next stained MVC-infected cells with DDAO to evaluate cell proliferation. Consistent with the cell death and cell cycle arrest induced during MVC infection, NS1-expressing cells showed a severely impaired proliferation of approximately 4-fold compared with NS1-negative cells both in early infection (3.8% versus 25.1% at 48 h p.i.) and later infection (18.8% versus 78.9% at 72 h p.i.) [Fig. 1D; compare groups NS(−) and NS+].

Taken together, these results show that MVC infection induces an apoptotic cell death and a perturbation of cell cycle progression from the S phase during early infection to the G_2/M phase during later infection.

MVC infection-induced apoptosis is mitochondrion mediated. We next sought to examine the potential activation of the mitochondrion-mediated apoptotic pathway in MVC infection-induced apoptosis. During mitochondrion-mediated apoptosis, the proapoptotic protein Bax translocalizes to the mitochondrion outer membrane to trigger the permeabilization of the outer membrane, which in turn results in cytochrome *c* release and downstream caspase activation (37). We first employed the MitoProbe $DiIC_1(5)$ to directly probe the level of mitochondrion outer membrane permeabilization (MOMP). During MVC infection, the degree of MOMP occurred in a time-dependent manner (Fig. 2A). NS1-expressing cells showed a clear transition from $DilC_1(5)^{high}/PI^-$ (live) to $DilC_1(5)^{low}/PI^-$ (early/middle apoptotic) and to $DilC_1(5)^{low}/PI^+$ (late apoptotic/dead) populations during infection from 48 to 96 h p.i. The $DilC_1(5)^{low}/PI^-$ population represents cells in which the mitochondrial outer membrane is disrupted but the cell membrane is intact, while the $DilC_1(5)^{low}/PI^+$ population represents cells in which both the mitochondrial outer membrane and the cell membrane are disrupted. This result indicated that MOMP precedes cell death during MVC infection.

We also costained MVC-infected cells with FAM-VAD-FMK (poly-FLICA) and $DilC_1(5)$ at 96 h p.i. The NS1-expressing cells showed three distinct populations as $DilC_1(5)^{high}/FLICA^-$ (nonapoptotic), $DilC_1(5)^{low}/FLICA^-$ (apoptosis initiating), and $DilC_1(5)^{low}/FLICA^+$ (apoptotic), respectively (Fig. 2B). The $DilC_1(5)^{low}/FLICA^-$ population represents cells in which the mitochondrial outer membrane is disrupted but caspases have not yet been activated, while the $DilC_1(5)^{low}/FLICA^+$ population represents cells with both a disrupted mitochondrial outer membrane and activated caspases. This result supports that a transition occurs from $DilC_1(5)$ staining to poly-FLICA staining in NS1-expressing cells. Collectively, these results suggest that MOMP precedes caspase activation and cell death during infection. The fact that caspases are activated in the same population of cells with MOMP is consistent with mitochondrion-mediated apoptosis.

To further confirm that MVC infection-induced apoptosis is mitochondrion mediated, we used anti-Bax staining and a mitochondrion-specific MitoRed staining to probe whether Bax localizes on the mitochondrial outer membrane. We observed a precise colocalization of the anti-Bax staining (green) with the MitoRed staining in MVC-infected cells at 48 h (Fig. 2C; MVC). In contrast, Bax dispersed in the uninfected cells (Fig. 2C; mock). This result indicates translocation of the Bax to the mitochondrial outer membrane of MVC-infected cells during infection, which presumably triggers disruption of the mitochondrial outer membrane potential that in turn activates caspases.

To confirm activation of individual caspases during infection, we used poly-FLICA and individual caspase FLICA assays to determine the level of activated caspases of NS1-expressing cells. Activation of caspases increased from 48 h, 72 h, and 96 h p.i.; however, at all three time points, similar patterns of caspase activation were detected (Fig. 2D). Among all the caspases tested, caspases 6, 8, and 9 were the most activated, followed by caspases 3/7, 10, and 12 (Fig. 2D). At 96 h p.i., while poly-FLICA showed an overall active caspase-positive rate of 58%, caspases 6, 8, and 9 were activated at rates of 53%, 53%, and 56% of NS1-expressing cells, respectively (Fig. 2D; 96 h). Active caspases 3/7, 10, and 12 were only detected in 40%, 43%, and 48% of NS1-expressing cells, respectively. The extensive activation of caspase 9 is further evidence that supports the mitochondrion-mediated apoptosis induced during MVC infection.

Replication of the MVC genome induces caspase activation. Next, we sought to explore which viral components were involved in MVC infection-induced apoptosis and cell cycle arrest. We transfected the MVC infectious clone, pIMVC, its derivatives pIMVCNS1(−), pIMVCNP1(−), pIMVCVP1(−), pIMVCVP2(−), pIMVCVP1/2(−), and pIMVCΔ1/2LTR and MVC NSCap gene-containing pMVCNSCap into WRD cells, separately. At 48 h posttransfection, we analyzed transfected cells for apoptosis and cell cycle by poly-FLICA and DAPI staining, respectively, and costained cells with anti-NS1, except for pIMVCNS1(−)-transfected cells, which were costained with anti-NP1. The NS1-expressing or NP1-expressing cells were then selected and plotted for FLICA or DAPI florescence intensity for comparison (Fig. 3A and B).

Transfection of pIMVC induced a 22% poly-$FLICA^+$ pop-

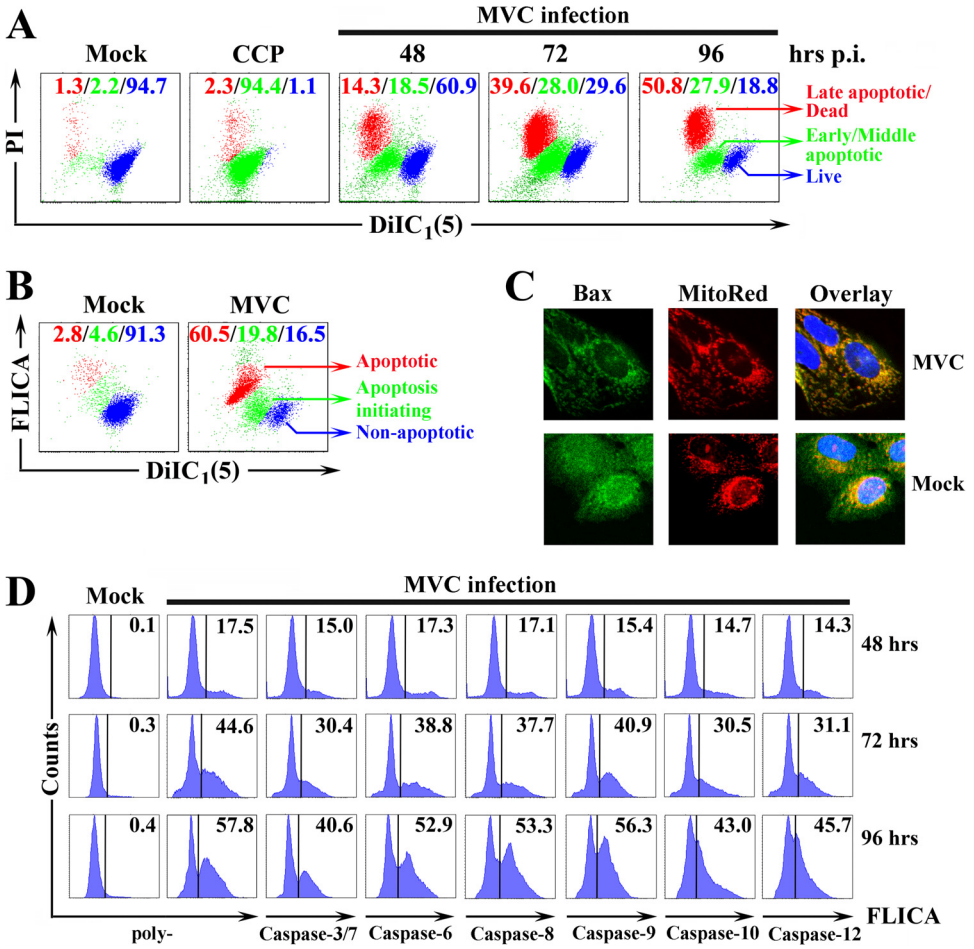

FIG. 2. MVC infection-induced apoptosis is mitochondrion mediated. WRD cells were infected with MVC at an MOI of 3. (A) MVC-infected cells were harvested at indicated times p.i. and double stained with PI and $DiIC_1(5)$. A mock infection control and an MOMP-positive control (CCCP-treated cells) were included. Stained cells were thereafter analyzed by flow cytometry and plotted as PI staining versus $DiIC_1(5)$ staining. The $DiIC_1(5)^{high}/PI^-$ (blue) population represents live cells; $DiIC_1(5)^{low}/PI^-$ (green) cells are in the early and middle stages of apoptosis; $DiIC_1(5)^{low}/PI^+$ (red) cells are late apoptotic or dead cells. The percentage of each cell population is shown in color. A representative of two independent experiments is shown. (B) MVC-infected WRD cells, at 96 h p.i., were double stained with poly-FLICA and $DiIC_1(5)$. A representative dot plot is shown. The $DiIC_1(5)^{high}/FLICA^-$ (blue) population represents live cells; the $DiIC_1(5)^{low}/FLICA^-$ (green) population are cells in the initial stage of apoptosis; the $DiIC_1(5)^{low}/FLICA^+$ (red) population are both apoptotic and dead cells. The percentage of each cell population is shown in color. (C) At 48 h p.i., mock- or MVC-infected WRD cells were stained with MitoTracker Red (red) and anti-Bax (green). Representative confocal images were taken. Nuclei were stained with DAPI. (D) At the indicated times p.i., MVC-infected WRD cells were stained with anti-NS1 and various FLICA peptides as shown. Anti-NS1-stained cells were selectively gated and plotted in histogram form to show the FLICA signals of NS1-expressing cells. Mock cells were all plotted as poly-FLICA staining. The percentage of FLICA positive cells is shown. A representative of two independent experiments is shown.

ulation in NS1-expressing cells at 48 h posttransfection (Fig. 3A; pIMVC). The NS1 knockout construct, pIMVCNS1(−), which is replication-deficient (60), generated only a 5.4% poly-$FLICA^+$ population [Fig. 3A; NS1(−)]. However, transfection of the NS(−) mutant did express NP1 that was used to select positive transfected cells, suggesting only expression of the NP1 does not activate caspases. The NP1 knockout construct, pIMVCNP1(−), which replicates poorly (60), generated a 9.8% poly-$FLICA^+$ population [Fig. 3A; NP1(−)]. Regardless of whether VP1, VP2, or both were knocked out, replication of the MVC genome was detected in pIMVCVP1(−)-, pIMVCVP2(−) (60)-, and pIMVCVP1/2(−)-transfected cells [Fig. 3C; VP1(−) and VP1/2(−)]; correspondingly, an average of 17% of $FLICA^+$ populations were detected in transfected cells [Fig. 3A; VP1(−), VP2(−), and VP1/2(−)]. Transfection of the half left terminal repeat (LTR)-deleted mutant, pIMVCΔ1/2LTR, of which replication was decreased (Fig. 3C; Δ1/2LTR), induced a reduced level (14%) of poly-$FLICA^+$ population (Fig. 3A; Δ1/2LTR). Transfection of the NSCap gene-containing construct, pMVCNSCap, which did not replicate (Fig. 3C; NSCap), failed to induce a significant level of poly-$FLICA^+$ population compared with the control (Fig. 3A; NSCap). However, transfection of the pMVCNSCap expressed NS1, which was used to select positive transfected cells, and NP1 (see Fig. 5B), suggesting that only expression of the NS1 and NP1 without replication of the genome does not activate caspases.

The VP1(−) and VP2(−) mutants have been shown to

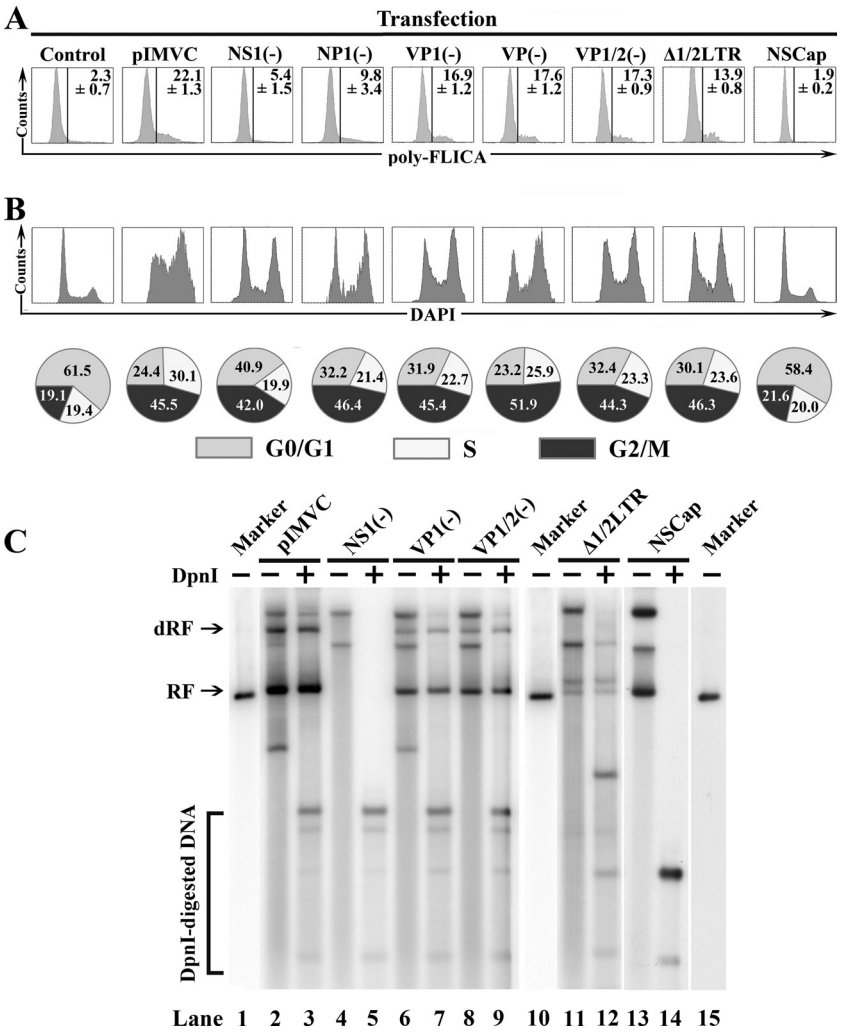

FIG. 3. Replication of the MVC genome activates caspases, and the MVC genome *per se* arrests cell cycle at the G_2/M phase. WRD cells were transfected with plasmids as shown. (A) At 48 h posttransfection, transfected cells were costained with anti-NS1, except for pIMVCNS1(−)-transfected cells, which were costained with anti-NP1 and poly-FLICA peptide. The anti-NS1-positive or anti-NP1-positive population was selectively gated and plotted as cell counts and FLICA signal. The percentage of FLICA-positive cells is shown as an average with a standard deviation generated from three independent experiments. (B) At 48 h posttransfection, transfected cells were costained with anti-NS1, except for pIMVCNS1(−)-transfected cells, which were costained with anti-NP1 and DAPI. Anti-NS1- or anti-NP1-stained cells were selectively gated and plotted as cell counts and DAPI signal. The percentage of each cell cycle phase was quantified and is shown as a pie graph at the bottom of the panel. A representative of two independent experiments is shown. (C) Southern blotting analysis of transfected WRD cells. At 48 h posttransfection, transfected cells were harvested and Hirt DNA was prepared. Hirt DNA was then digested with DpnI. The blot was probed with the NSCap probe as previously described (60). Detected bands are indicated with their respective designations to the left. Lanes 1, 10, and 15 are size markers of 5.15 kb. RF, replicative form; dRF, double replicative form.

knock out VP1 and VP2 expression by a single burst replication of the viral genome (60). Transfection of the combined VP1/2(−) mutant resulted in a single burst replication compared with transfection of the VP1(−) mutant [Fig. 3C; compare VP1/2(−) with VP1(−)]. These results suggest that without expression of VP1 and VP2, only replication of the MVC genome is sufficient to activate caspases.

Replication efficiency of these transfected constructs as shown by Southern blots was ranked as pIMVC > pIMVCVP1(−), pIMVCVP2(−), and pIMVCVP1/2(−) > pIMVCΔ1/2LTR > pIMVCNS1(−) and pMVCNSCap (Fig. 3C). Thus, the efficiency of replication seems to correlate directly with the level of caspase activation. Collectively, these results reveal that activation of caspases, as assayed by poly-FLICA, of transfected cells is associated with replication of the MVC genome, rather than the expression of the MVC NP1 and VP1/VP2 capsid proteins.

The MVC genome *per se* arrests the cell cycle at the G_2/M phase. With DAPI-staining, we further examined the capability of inducing cell cycle arrest through transfection of these MVC constructs. Transfection of the infectious clone (pIMVC) induced a scenario of cell cycle arrest at the G_2/M phase similar to that of MVC-infected cells with a transition of S-phase accumulation (Fig. 3B; pIMVC). Surprisingly, at 48 h posttransfection, cells transfected with pIMVCNS1(−), pIMVCNP1(−), pIMVCVP1(−), pIMVCVP2(−), and

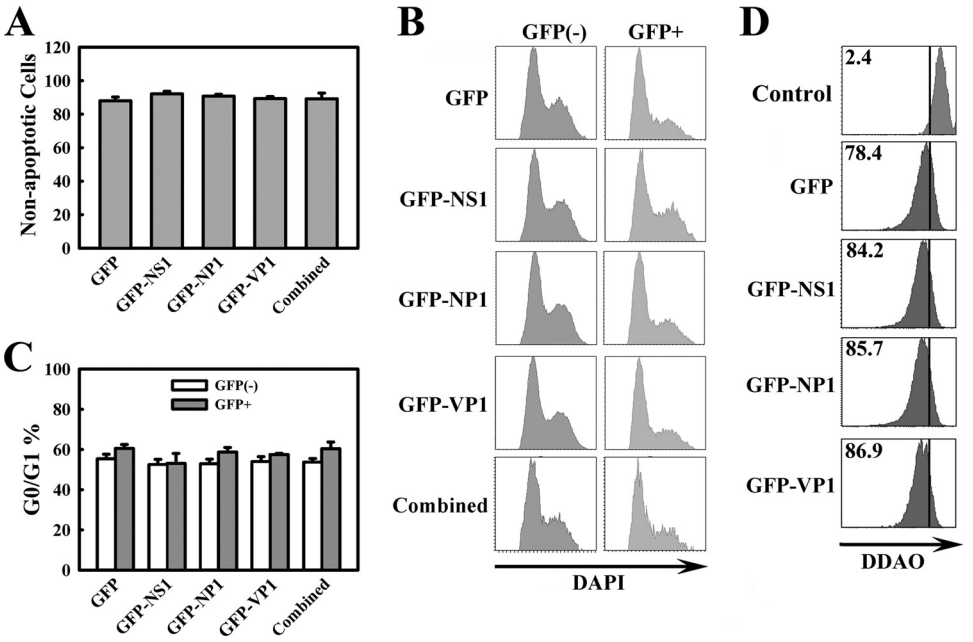

FIG. 4. Expression of individual MVC proteins or in combination by transfection does not induce cell death or cell cycle arrest. WRD cells were transfected with various constructs, as shown, that express GFP-fused MVC proteins. (A) Transfected cells were costained with annexin V-PI at 48 h posttransfection. The GFP-positive population was selectively gated. The percentage of nonapoptotic cells (annexin V^-/PI^- population) in the GFP-positive population in each transfection was then plotted. All the values were generated from three independent experiments and are shown as an average with a standard deviation. (B) Representative results of cell cycle analysis. Transfected cells were stained with DAPI at 48 h posttransfection. The GFP-positive population was selectively gated. The cell cycle analysis results are shown as GFP-negative population versus GFP-positive population. (C)The percentage of cells at the G_0/G_1 phase is shown as an average with a standard deviation obtained from three independent experiments. (D) Transfected cells were stained with DDAO at 48 h posttransfection. The GFP-positive population was selectively gated and plotted. Numbers as shown are percentages of proliferated cells. The line as shown is arbitrarily set in the control cells, which were fixed immediately after transfection.

pIMVCVP1/2(−), which all contain terminal repeats at both ends, showed apparent G_2/M arrests of approximately 42%, 46%, 45%, 52%, and 44%, respectively, in comparison with 19% in the control group (Fig. 3B). However, no apparent S-phase accumulation was observed in cells transfected with the above pIMVC mutants, even at earlier time points (data not shown). Interestingly, transfection of the left half terminal repeat (TR)-deleted mutant, pIMVCΔ1/2LTR, still induced a G_2/M arrest of 46% (Fig. 3B, Δ1/2LTR); however, transfection of the TR-deleted mutant pMVCNSCap failed to induce G_2/M arrest in NS1-expressing cells compared with the control (Fig. 3B; NSCap).

Together with those results from Southern blotting analysis (Fig. 3C), our observations suggest that the terminal repeats of the MVC genome are required to induce cell cycle arrest at the G_2/M phase, and replication of the genome and expression of the NS1, NP1, and VP1/2 proteins are dispensable. The S-phase accumulation as seen during MVC infection and transfection of the infectious clone may require a status of efficient replication of the viral genome.

Expression of MVC individual viral proteins by transfection does not induce cell death or cell cycle arrest. To further confirm that MVC proteins are not required to induce apoptosis and cell cycle arrest of transfected WRD cells, we transfected WRD cells with a set of constructs expressing GFP-fused MVC proteins, and the GFP-positive population was selectively gated and quantified by annexin V staining for apoptosis (16). Not surprisingly, no significant amount of apoptosis or cell cycle disturbance was observed in cells transfected with individual or combined GFP-fused MVC protein-expressing constructs in comparison with cells transfected with the GFP control, as shown by annexin V-PI staining for apoptosis (Fig. 4A) and DAPI staining for cell cycle (Fig. 4B and C).

Expression of these GFP-fused proteins by transfection was confirmed by fluorescence microscopy (Fig. 5A); approximately 10% of WRD cells were GFP positive. GFP-NS1 and -NP1 showed a similar nucleus localization to that of the wild-type NS1 and NP1 expressed from the transfection of pMVCNSCap in WRD cells (Fig. 5B), while transfection of the GFP-VP1 showed localization mostly in the nucleus, with some diffusion in the cytoplasm (Fig. 5A). Interestingly, during MVC infection, the NS1 was localized in distinct replication center-like foci (Fig. 5B; MVC/α-NS1), similar to that of other parvoviruses (9, 59), while the NP1 showed a unique perinucleus localization (Fig. 5B; MVC/α-NP1). The pattern of NS1 localization was also observed in cells transfected with replicative pIMVC and pIMVCVP1/2(−) (Fig. 5B). We speculate that the unique localization of the NS1 is due to the replication of the viral genome. Transfection of the pIMVCNP1(−) and pMVCNSCap did not show clear NS1-localized foci in the nucleus (Fig. 5B). We did not observe the perinucleus localization of NP1 in cells transfected with both replicative and nonreplicative MVC constructs (Fig. 5B). Thus, we believe that the difference in the localization pattern

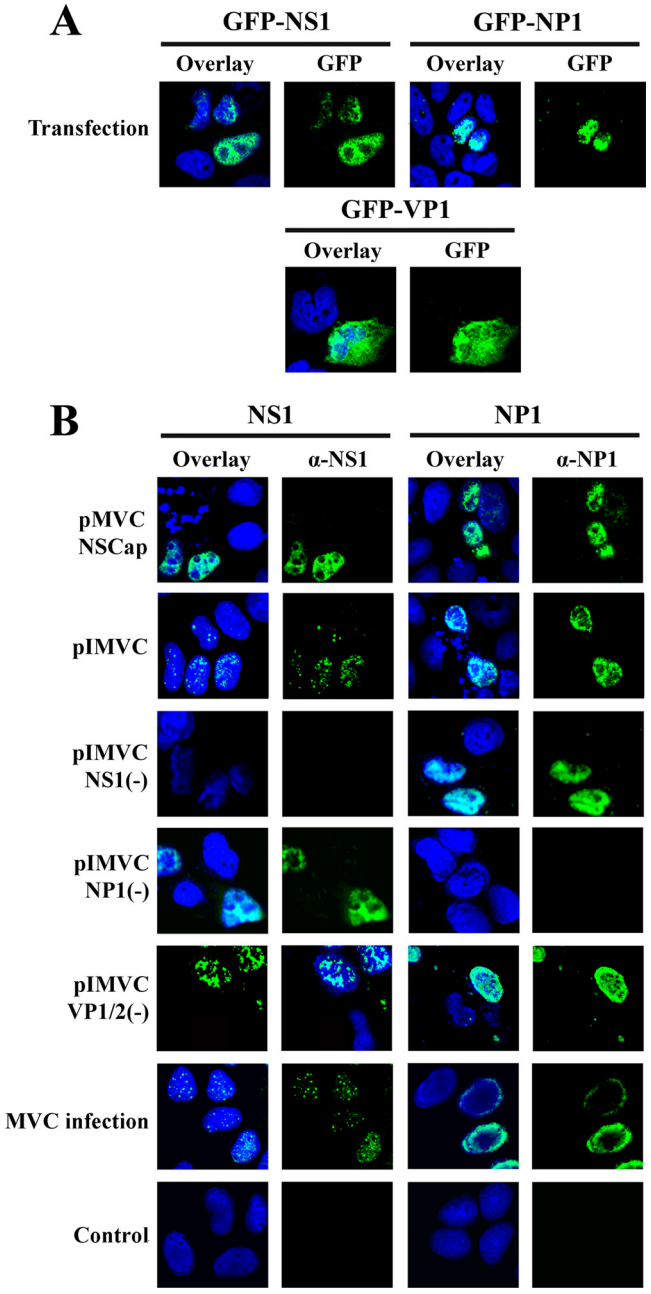

FIG. 5. Cellular localization of MVC proteins during infection and in transfection. (A) WRD cells were transfected with constructs expressing GFP-fused MVC proteins as shown. Cells were treated at 48 h posttransfection. (B) WRD cells were infected with MVC at an MOI of 3 or transfected with the MVC constructs as indicated. At 48 h p.i. or posttransfection, cells were stained with anti-NS1 (α-NS1) and anti-NP1 (α-NP1), respectively. Confocal images were taken at ×60 magnification. Nuclei were stained with DAPI.

of the NS1 and NP1 in the nucleus is less likely to result in the inability of the NS1 and NP1 to induce apoptosis. In addition to these observations, we also observed that expression of individual GFP-fused MVC proteins or those combined by transfection did not inhibit cell proliferation compared with that in the control GFP transfection group (Fig. 4D).

Collectively, our results suggest that unlike the nonstructural proteins of other parvoviruses, the MVC proteins, especially NS1 and NP1, expressed by transfection of WRD cells, do not induce an apparent cell death or a perturbation of cell cycle progression.

UV-inactivated MVC induces cell cycle arrest but not cell death. To further confirm the role of the MVC genome in inducing apoptosis and cell cycle arrest, we inactivated purified MVC by UV irradiation. WRD cells were either infected with untreated (MVC) or inoculated with UV-irradiated MVC (UV-MVC). Apoptosis and cell cycle status were evaluated by Live/Dead Violet-FLICA costaining and DAPI staining, respectively. Since NS1 was not expressed in WRD cells inoculated with UV-MVC (data not shown), we used an MOI of 9 for inoculation. We gated total cells and plotted them in Fig. 6A and B. At this MOI, MVC infection induced apoptosis more drastically, which was observed as early as 18 h p.i. and progressed over the course of infection (Fig. 6A; MVC). At 48 h p.i., only 46% of MVC-infected cells were still alive (Live/Dead Violet$^-$/FLICA$^-$). In contrast, UV-MVC inoculation failed to induce a significant level of cell death at all three times p.i. (Fig. 6A; UV-MVC).

Meanwhile, we compared the cell cycle regulation of MVC-infected and UV-MVC-inoculated WRD cells at the same MOI. Consistent with the findings shown in Fig. 1B, the S-phase accumulation transitioned to the G_2/M arrest during MVC infection (Fig. 6B; MVC). While most of the WRD cells were at the S phase at 18 h p.i., the majority of MVC-infected cells were arrested at the G_2/M phase at late time points. Interestingly, UV-MVC induced a significant cell cycle arrest at G_2/M as early as 18 h p.i. (Fig. 6B; UV-MVC). Consistent with the transfection experiments shown in Fig. 3, we did not observe an S-phase accumulation during UV-MVC inoculation (Fig. 6B). Moreover, to confirm the G_2/M arrest induced by UV-MVC inoculation, we determined the protein level of the G_2/M-phase checkpoint regulators in UV-MVC-inoculated cells. A significant increase of both cyclin B1 and cdc2 (pY15) was observed at both 18 and 24 h p.i. (Fig. 6C). However, the fold of increase was less than that of the MVC-infected cells shown in Fig. 1C. The level of cyclin A remained unchanged in UV-MVC-inoculated cells.

Collectively, these lines of evidence further support that the MVC viral genome alone can induce cell cycle arrest at the G_2/M phase but not the S-phase accumulation or cell death.

DISCUSSION

***Bocavirus* MVC infection induces a mitochondrion-mediated apoptosis.** Parvovirus infection often causes cell death of infected cells either by apoptosis or by various mechanisms of nonapoptotic cell death. Novel mechanisms of nonapoptotic cell death induced by parvovirus infection have been revealed recently. MVM infection-induced cell death is mediated by NS1 interference with intracellular CKII signaling (22, 44, 45). On the other hand, parvovirus H-1 can induce a nonapoptotic cell death of glioma cells that is dependent on accumulation of cathepsin B/L (25). However, the mechanisms underlying parvovirus infection-induced apoptosis have not been elucidated in detail. Apoptosis is defined mechanistically as three pathways of regulated cell death involving the sequential activation of caspases, the extrinsic pathway is involved in the engage-

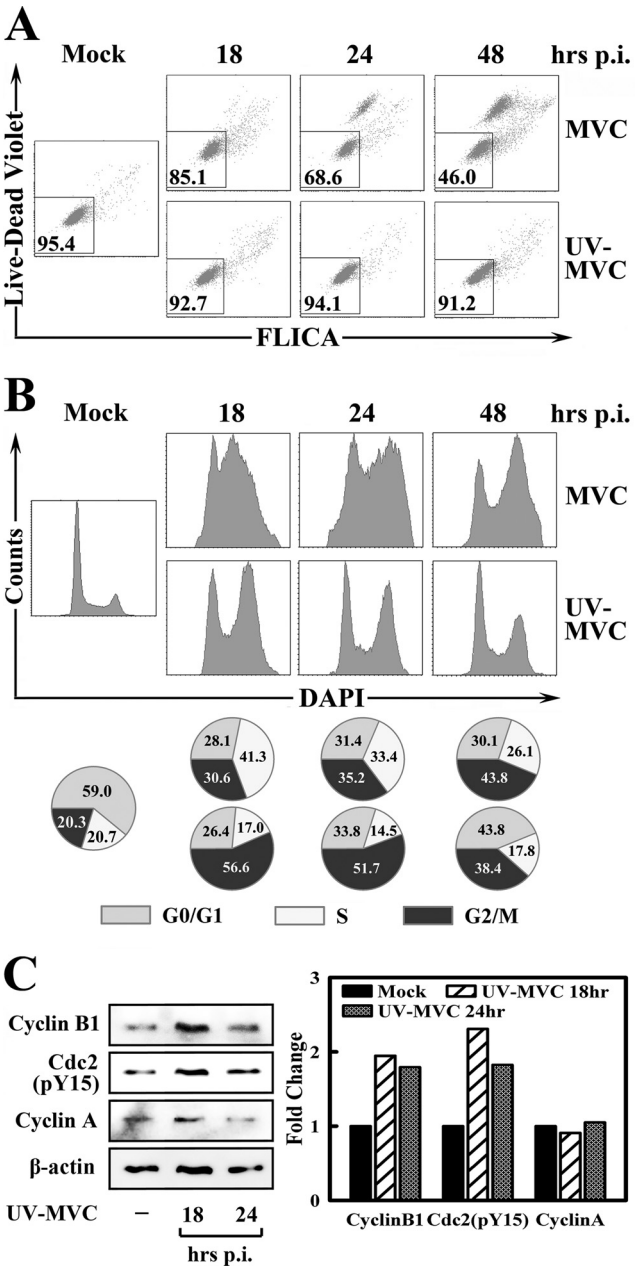

FIG. 6. UV-MVC inoculation induces cell cycle arrest at G_2/M but not cell death. WRD cells were infected by MVC or inoculated with UV-MVC at an MOI of 9. (A) Infected or inoculated cells were costained with Live/Dead Violet and poly-FLICA peptide at indicated times p.i. Stained cells were plotted in histograms as Live/Dead Violet and FLICA signals. The numbers in the square show percentages of live cells (double negative). (B) At 48 h p.i., mock- or UV-MVC-infected cells were stained with DAPI and plotted as cell counts and DAPI signal. The percentage of each cell cycle phase was quantified and is shown as a pie graph at the bottom of the panel. (C) UV-MVC-infected cells were harvested at indicated times p.i. Cell lysates were subjected to Western blotting analysis using anti-cyclin B1, anti-cdc2 (pY15), anti-cyclin A, and anti-β-actin, respectively. The level of signals on blots is normalized to the level of β-actin and is shown in the bar chart. The normalized value of the mock cells is arbitrarily set to 1. A representative of two independent experiments is shown in panels A and B.

ment of particular "death" receptors (e.g., Fas) and through the formation of the death-inducing signaling complex (DISC) (8). The mitochondrion-mediated (intrinsic) pathway is activated by "BH3-only" proteins such as tBid, Bad, Bim, and PUMA; these activated proteins are subsequently translocated to the mitochondrial membrane, where they activate the proapoptotic proteins Bax and Bak (37). Bax/Bak activation results in mitochondrial outer membrane permeabilization (MOMP), with consequent release of cytochrome *c* and other mitochondrial proteins with the consequent activation of caspase 9 (18). Activated caspase 8/10 is also able to cleave Bid to tBid, which activates Bax/Bak. In endoplasmic reticulum (ER)-stress-mediated apoptosis, caspase 12 is localized to the ER and activated by ER stress (43).

We have shown in our studies that MVC infection induces an apoptotic cell death, represented by the presence of activated caspases in infected cells. Consistently, the specific pancaspase inhibitor Q-VD completely blocked MVC infection-induced cell death. Moreover, the translocalization of the proapoptotic Bax to the mitochondrial outer membrane and consequently the time-dependent disruption of mitochondrial outer membrane potential indicated the activation of mitochondrion-mediated apoptosis during MVC infection. This mechanism is further supported by the extensive activation of caspases, especially the activated caspase 9, during MVC infection. We also detected the activation of the initiator caspases 8, 10, and 12; however, whether the extrinsic pathway or the ER-stress-mediated pathway is also involved in MVC infection-induced apoptosis to some extent warrants further investigation.

Replication of the viral genome induces apoptosis of MVC-infected cells. In our results, expression of the nonstructural protein NS1 and NP1 of MVC did not induce cell death in transfected cells, which contrasts with the function of the large nonstructural protein of other parvoviruses, e.g., the NS1 of MVM (44), H-1 (52), and B19V (58), the Rep78 of adeno-associated virus type 2 (AAV2) (56), and the small nonstructural protein 11kDa of B19V (16). Thus, our results suggest that the noncytotoxic nature of the MVC NS1 is novel in parvoviruses and might be a general feature of the NS1 among other members in the genus *Bocavirus*.

Surprisingly, our studies showed that activation of caspases coincided with the replication of the viral gnome. The efficiency of replication correlated well with the level of caspase activation in cells transfected with pIMVC and its mutants (Fig. 3A and C). In the scenario in which replication of the MVC genome occurs either during MVC infection or in transfection of the replicative MVC constructs, apoptosis is induced in infected or transfected cells. However, when DNA replication is abolished either by knocking out NS1 expression or by deleting both terminal repeats, transfection of these nonreplicative mutants does not induce apoptosis. When DNA replication is significantly reduced either by knocking out the NP1 expression or deleting the left half terminal repeats, transfection of these replication-reduced mutants induces a decreased degree of apoptosis. These observations strongly suggest that the apoptosis induced from transfection of the MVC infectious clone and its replicative derivatives is dependent on the replication of the MVC genome. We know that only expression of the viral proteins by transfection (Fig. 4) does not induce

apoptosis; however, NS1 is essential for the replication of the viral genome. Thus, we cannot rule out an indirect role of the NS1 in inducing apoptosis during MVC infection.

It is reasonable to speculate that a DNA damage response could be induced in WRD cells upon MVC infection or simply by replication of the viral genome. A DNA damage response induced by AAV2 infection has been extensively explored (51, 61, 64). AAV2 DNA, which is single stranded with hairpin loops at both ends, can be sensed as abnormal DNA by the cell, triggering a DNA damage response independent of p53 (51). We have evidence that MVC infection induced a DNA damage response represented by phosphorylation of H2AX, p53, and ATM (data not shown). The DNA damage response induces apoptosis when the damage is not repairable through upregulation of the proapoptotic proteins such as tBid, Fas, Bax, or PUMA (5, 35, 54). It is also possible that an initial DNA damage response induced by the MVC genome incurs cell cycle arrest, and later, during viral DNA replication, accumulated MVC genomes trigger an irreversible DNA damage response that results in apoptotic cell death. On the other hand, the DNA damage response signals the DNA repair machinery, which may be helpful in replicating the single-stranded genome of MVC. These novel mechanisms have never been studied in autonomous parvovirus infection and warrant further investigation. Therefore, we have provided an excellent model to study how the viral genome and its replication induce cellular responses that favor virus DNA replication at an early stage of infection and egress of progeny virus at a later stage of infection. The apoptosis induced by replication of the MVC genomes may be a common mechanism underlying parvovirus infection-induced apoptosis.

***Bocavirus* MVC infection induces cell cycle arrest.** Parvovirus infection induces cell cycle arrest (30, 33, 42, 47, 65), most often at the S/G_2 phase, which favors virus DNA replication. However, a G_2/M-phase arrest is clearly observed as early as 6 h after B19V infection (42). Nevertheless, we have shown here that MVC infection incurs an apparent S-phase accumulation at early infection followed by an arrest of the G_2/M phase in late infection (Fig. 1). The DAPI staining in our study presents the authentic cell cycle of host cells. We quantified the MVC genomic copy number per cell at 48 h p.i. The genomic copy number per cell, which includes the replicative form (RF) DNA of MVC, was approximately 0.1 million, which equals 0.55 billion bases. The human genome contains approximately 3.4 billion base pairs per cell (http://www.genome.gov/18016863). Thus, assuming the canine genome is similar in size to the human genome, the DAPI staining contributed by the replicated MVC genomes and RF DNA is less than 8% of the total DAPI staining in an infected cell, which is not sufficient to change the pattern of the cell cycle represented by DAPI staining. Based on evidence showing the critical cell cycle proteins and inhibition of cell proliferation during MVC infection (Fig. 1C and D), we believe that the DAPI staining presents the authentic cell cycle of MVC-infected cells in our studies.

Cell cycle arrest at the G_2/M phase often precedes the onset of apoptosis (23, 31, 63). We did not observe an apparent G_2/M-phase arrest preceding apoptosis during MVC infection. In contrast, G_2/M arrest by transfection of the NS1-knockout mutant [pMVCNS1(−)] or UV-irradiated MVC did not induce apoptosis (Fig. 3 and 6), and inhibition of apoptosis by Q-VD did not release cell cycle arrest (data not shown). Thus, we believe that the cell cycle arrest and apoptosis of MVC infection are induced through independent pathways in parallel.

In transfecting the mutant MVC infectious clones, as shown in Fig. 3, we tested cell cycle arrest at early time points of transfection. We were not able to detect any S-phase accumulation in transfection of these mutants other than the infectious clone *per se* (data not shown). Nevertheless, we consistently observed the G_2/M arrest at 48 h posttransfection in all the transfections of the mutant infectious clones that contain the viral terminal repeats. Thus, the S-phase accumulation appears only when highly efficient replication occurs: e.g., transfection of the infectious clone or MVC infection. The S phase has been emphasized to be important for parvovirus replication. For example, parvovirus H-1 protein synthesis coincides with cellular DNA synthesis (62), and MVM replication apparently requires mitotically active cells (28). Efficient replication of the MVC genome could possibly trigger the S-phase accumulation which loops back to further facilitate MVC DNA replication.

The genome of MVC induces cell cycle arrest at G_2/M. Using UV-MVC, we were able to show a significant level of G_2/M arrest of UV-MVC-inoculated WRD cells as early as 18 h p.i. UV-MVC infection-induced cell cycle arrest at G_2/M is consistent with previous reports of other parvoviruses (41, 51, 53). The genome of AAV2 that contains an identical inverted terminal repeat at both ends has been shown to induce cell cycle arrest at the G_2/M phase (51). Infection of UV-irradiated B19V has been shown to induce a G_2/M arrest as early as at 24 h p.i. (41). The G_2/M-phase arrest by the MVC genome alone was also reproduced by transfection of the NS1 knockout mutant of the MVC infectious clone. The MVC genome that lacks half of the left terminal repeat still induced a clear G_2/M arrest by transfection. Only the MVC genome that does not contain both terminal repeats, the NSCap gene, lost its ability to induce cell cycle arrest. These observations suggest that the terminal repeats of the MVC genome, which form strong secondary structures (60), play an important role in inducing cell cycle arrest at the G_2/M-phase during MVC infection. It may be true that the structure of the terminal repeats of parvoviruses acts as a perfect trigger to induce DNA damage response, which in turn, induces cell cycle arrest.

ACKNOWLEDGMENTS

This work was supported by PHS grant RO1 AI070723 from NIAID and grant P20 RR016443 from the NCRR COBRE program.

We thank Joyce G. Slusser at the Flow Cytometry Core for valuable discussions. We thank Colin Parrish at the James A. Baker Institute, Cornell University, and David Pintel at the Life Sciences Center, University of Missouri—Columbia, for valuable reagents.

REFERENCES

1. **Abdel-Latif, L., B. K. Murray, R. L. Renberg, K. L. O'Neill, H. Porter, J. B. Jensen, and F. B. Johnson.** 2006. Cell death in bovine parvovirus-infected embryonic bovine tracheal cells is mediated by necrosis rather than apoptosis. J. Gen. Virol. **87:**2539–2548.
2. **Allander, T.** 2008. Human bocavirus. J. Clin. Virol. **41:**29–33.
3. **Allander, T., T. Jartti, S. Gupta, H. G. Niesters, P. Lehtinen, R. Osterback, T. Vuorinen, M. Waris, A. Bjerkner, A. Tiveljung-Lindell, B. G. van den Hoogen, T. Hyypia, and O. Ruuskanen.** 2007. Human bocavirus and acute wheezing in children. Clin. Infect. Dis. **44:**904–910.
4. **Allander, T., M. T. Tammi, M. Eriksson, A. Bjerkner, A. Tiveljung-Lindell,**

and B. Andersson. 2005. Cloning of a human parvovirus by molecular screening of respiratory tract samples. Proc. Natl. Acad. Sci. U. S. A. **102:**12891–12896.

5. **Andersen, J. L., E. S. Zimmerman, J. L. DeHart, S. Murala, O. Ardon, J. Blackett, J. Chen, and V. Planelles.** 2005. ATR and GADD45alpha mediate HIV-1 Vpr-induced apoptosis. Cell Death Differ. **12:**326–334.
6. **Anouja, F., R. Wattiez, S. Mousset, and P. Caillet-Fauquet.** 1997. The cytotoxicity of the parvovirus minute virus of mice nonstructural protein NS1 is related to changes in the synthesis and phosphorylation of cell proteins. J. Virol. **71:**4671–4678.
7. **Arthur, J. L., G. D. Higgins, G. P. Davidson, R. C. Givney, and R. M. Ratcliff.** 2009. A novel bocavirus associated with acute gastroenteritis in Australian children. PLoS. Pathog. **5:**e1000391.
8. **Ashkenazi, A., and V. M. Dixit.** 1998. Death receptors: signaling and modulation. Science **281:**1305–1308.
9. **Bashir, T., J. Rommelaere, and C. Cziepluch.** 2001. In vivo accumulation of cyclin A and cellular replication factors in autonomous parvovirus minute virus of mice-associated replication bodies. J. Virol. **75:**4394–4398.
10. **Binn, L. N., E. C. Lazar, G. A. Eddy, and M. Kajima.** 1970. Recovery and characterization of a minute virus of canines. Infect. Immun. **1:**503–508.
11. **Binn, L. N., R. H. Marchwicki, E. H. Eckermann, and T. E. Fritz.** 1981. Viral antibody studies of laboratory dogs with diarrheal disease. Am. J. Vet. Res. **42:**1665–1667.
12. **Bloom, M. E., R. E. Race, and J. B. Wolfinbarger.** 1980. Characterization of Aleutian disease virus as a parvovirus. J. Virol. **35:**836–843.
13. **Brandenburger, A., D. Legendre, B. Avalosse, and J. Rommelaere.** 1990. NS-1 and NS-2 proteins may act synergistically in the cytopathogenicity of parvovirus MVMp. Virology **174:**576–584.
14. **Carmichael, L. E., D. H. Schlafer, and A. Hashimoto.** 1991. Pathogenicity of minute virus of canines (MVC) for the canine fetus. Cornell Vet. **81:**151–171.
15. **Chauvier, D., S. Ankri, C. Charriaut-Marlangue, R. Casimir, and E. Jacotot.** 2007. Broad-spectrum caspase inhibitors: from myth to reality? Cell Death Differ. **14:**387–391.
16. **Chen, A. Y., E. Y. Zhang, W. Guan, F. Cheng, S. Kleiboeker, T. M. Yankee, and J. Qiu.** 2010. The small 11kDa non-structural protein of human parvovirus B19 plays a key role in inducing apoptosis during B19 virus infection of primary erythroid progenitor cells. Blood **115:**1070–1080.
17. **Chen, K. C., B. C. Shull, E. A. Moses, M. Lederman, E. R. Stout, and R. C. Bates.** 1986. Complete nucleotide sequence and genome organization of bovine parvovirus. J. Virol. **60:**1085–1097.
18. **Chen, M., and J. Wang.** 2002. Initiator caspases in apoptosis signaling pathways. Apoptosis **7:**313–319.
19. **Chen, Z., W. Guan, F. Cheng, A. Y. Chen, and J. Qiu.** 2009. Molecular characterization of human parvovirus B19 genotypes 2 and 3. Virology **394:**276–285.
20. **Cheng, F., A. Y. Chen, S. M. Best, M. E. Bloom, D. Pintel, and J. Qiu.** 2010. The capsid proteins of Aleutian mink disease virus (AMDV) activate caspases and are specifically cleaved during infection. J. Virol. **84:**2687–2696.
21. **Cotmore, S. F., and P. Tattersall.** 2005. Structure and organization of the viral genome, p. 73–94. *In* J. Kerr, S. F. Cotmore, M. E. Bloom, R. M. Linden, and C. R. Parrish (ed.), Parvoviruses. Hodder Arnold, London, United Kingdom.
22. **Daeffler, L., R. Horlein, J. Rommelaere, and J. P. Nuesch.** 2003. Modulation of minute virus of mice cytotoxic activities through site-directed mutagenesis within the NS coding region. J. Virol. **77:**12466–12478.
23. **D'Agnillo, F., and A. I. Alayash.** 2001. Redox cycling of diaspirin cross-linked hemoglobin induces G2/M arrest and apoptosis in cultured endothelial cells. Blood **98:**3315–3323.
24. **Degterev, A., M. Boyce, and J. Yuan.** 2003. A decade of caspases. Oncogene **22:**8543–8567.
25. **Di Piazza, M., C. Mader, K. Geletneky, Y. C. Herrero, E. Weber, J. Schlehofer, L. Deleu, and J. Rommelaere.** 2007. Cytosolic activation of cathepsins mediates parvovirus H-1-induced killing of cisplatin and TRAIL-resistant glioma cells. J. Virol. **81:**4186–4198.
26. **Fragkos, M., J. Jurvansuu, and P. Beard.** 2009. H2AX is required for cell cycle arrest via the p53/p21 pathway. Mol. Cell. Biol. **29:**2828–2840.
27. **Guan, W., F. Cheng, Y. Yoto, S. Kleiboeker, S. Wong, N. Zhi, D. J. Pintel, and J. Qiu.** 2008. Block to the production of full-length B19 virus transcripts by internal polyadenylation is overcome by replication of the viral genome. J. Virol. **82:**9951–9963.
28. **Guetta, E., D. Ron, and J. Tal.** 1986. Development-dependent replication of minute virus of mice in differentiated mouse testicular cell lines. J. Gen. Virol. **67:**2549–2554.
29. **Harrison, L. R., E. L. Styer, A. R. Pursell, L. E. Carmichael, and J. C. Nietfeld.** 1992. Fatal disease in nursing puppies associated with minute virus of canines. J. Vet. Diagn. Invest. **4:**19–22.
30. **Hermanns, J., A. Schulze, D. Jansen, J. A. Kleinschmidt, R. Schmidt, and H. zur Hausen.** 1997. Infection of primary cells by adeno-associated virus type 2 results in a modulation of cell cycle-regulating proteins. J. Virol. **71:**6020–6027.
31. **Ito, K., T. Nakazato, Y. Miyakawa, K. Yamato, Y. Ikeda, and M. Kizaki.** 2003. Caffeine induces G2/M arrest and apoptosis via a novel p53-dependent pathway in NB4 promyelocytic leukemia cells. J. Cell Physiol. **196:**276–283.
32. **Jarplid, B., H. Johansson, and L. E. Carmichael.** 1996. A fatal case of pup infection with minute virus of canines (MVC). J. Vet. Diagn. Invest. **8:**484–487.
33. **Jurvansuu, J., K. Raj, A. Stasiak, and P. Beard.** 2005. Viral transport of DNA damage that mimics a stalled replication fork. J. Virol. **79:**569–580.
34. **Kahn, J.** 2008. Human bocavirus: clinical significance and implications. Curr. Opin. Pediatr. **20:**62–66.
35. **Kamer, I., R. Sarig, Y. Zaltsman, H. Niv, G. Oberkovitz, L. Regev, G. Haimovich, Y. Lerenthal, R. C. Marcellus, and A. Gross.** 2005. Proapoptotic BID is an ATM effector in the DNA-damage response. Cell **122:**593–603.
36. **Kapoor, A., E. Slikas, P. Simmonds, T. Chieochansin, A. Naeem, S. Shaukat, M. M. Alam, S. Sharif, M. Angez, S. Zaidi, and E. Delwart.** 2009. A newly identified bocavirus species in human stool. J. Infect. Dis. **199:**196–200.
37. **Kim, H., H. C. Tu, D. Ren, O. Takeuchi, J. R. Jeffers, G. P. Zambetti, J. J. Hsieh, and E. H. Cheng.** 2009. Stepwise activation of BAX and BAK by tBID, BIM, and PUMA initiates mitochondrial apoptosis. Mol. Cell **36:**487–499.
38. **Lytle, C. D., and J. L. Sagripanti.** 2005. Predicted inactivation of viruses of relevance to biodefense by solar radiation. J. Virol. **79:**14244–14252.
39. **Mochizuki, M., M. Hashimoto, T. Hajima, M. Takiguchi, A. Hashimoto, Y. Une, F. Roerink, T. Ohshima, C. R. Parrish, and L. E. Carmichael.** 2002. Virologic and serologic identification of minute virus of canines (canine parvovirus type 1) from dogs in Japan. J. Clin. Microbiol. **40:**3993–3998.
40. **Moehler, M., B. Blechacz, N. Weiskopf, M. Zeidler, W. Stremmel, J. Rommelaere, P. R. Galle, and J. J. Cornelis.** 2001. Effective infection, apoptotic cell killing and gene transfer of human hepatoma cells but not primary hepatocytes by parvovirus H1 and derived vectors. Cancer Gene Ther. **8:**158–167.
41. **Morita, E., A. Nakashima, H. Asao, H. Sato, and K. Sugamura.** 2003. Human parvovirus B19 nonstructural protein (NS1) induces cell cycle arrest at G_1 phase. J. Virol. **77:**2915–2921.
42. **Morita, E., K. Tada, H. Chisaka, H. Asao, H. Sato, N. Yaegashi, and K. Sugamura.** 2001. Human parvovirus B19 induces cell cycle arrest at G_2 phase with accumulation of mitotic cyclins. J. Virol. **75:**7555–7563.
43. **Nakagawa, T., H. Zhu, N. Morishima, E. Li, J. Xu, B. A. Yankner, and J. Yuan.** 2000. Caspase-12 mediates endoplasmic-reticulum-specific apoptosis and cytotoxicity by amyloid-beta. Nature **403:**98–103.
44. **Nuesch, J. P., and J. Rommelaere.** 2006. NS1 interaction with CKII alpha: novel protein complex mediating parvovirus-induced cytotoxicity. J. Virol. **80:**4729–4739.
45. **Nuesch, J. P., and J. Rommelaere.** 2007. A viral adaptor protein modulating casein kinase II activity induces cytopathic effects in permissive cells. Proc. Natl. Acad. Sci. U. S. A. **104:**12482–12487.
46. **Op De Beeck, A., F. Anouja, S. Mousset, J. Rommelaere, and P. Caillet-Fauquet.** 1995. The nonstructural proteins of the autonomous parvovirus minute virus of mice interfere with the cell cycle, inducing accumulation in G2. Cell Growth Differ. **6:**781–787.
47. **Op De Beeck, A., J. Sobczak-Thepot, H. Sirma, F. Bourgain, C. Brechot, and P. Caillet-Fauquet.** 2001. NS1- and minute virus of mice-induced cell cycle arrest: involvement of p53 and p21(cip1). J. Virol. **75:**11071–11078.
48. **Pintel, D., D. Dadachanji, C. R. Astell, and D. C. Ward.** 1983. The genome of minute virus of mice, an autonomous parvovirus, encodes two overlapping transcription units. Nucleic Acids Res. **11:**1019–1038.
49. **Pratelli, A., D. Buonavoglia, M. Tempesta, F. Guarda, L. Carmichael, and C. Buonavoglia.** 1999. Fatal canine parvovirus type-1 infection in pups from Italy. J. Vet. Diagn. Invest. **11:**365–367.
50. **Qiu, J., A. Handa, M. Kirby, and K. E. Brown.** 2000. The interaction of heparin sulfate and adeno-associated virus 2. Virology **269:**137–147.
51. **Raj, K., P. Ogston, and P. Beard.** 2001. Virus-mediated killing of cells that lack p53 activity. Nature **412:**914–917.
52. **Rayet, B., J. A. Lopez-Guerrero, J. Rommelaere, and C. Dinsart.** 1998. Induction of programmed cell death by parvovirus H-1 in U937 cells: connection with the tumor necrosis factor alpha signalling pathway. J. Virol. **72:**8893–8903.
53. **Rommelaere, J., and D. C. Ward.** 1982. Effect of UV-irradiation on DNA replication of the parvovirus minute-virus-of-mice in mouse fibroblasts. Nucleic Acids Res. **10:**2577–2596.
54. **Roos, W. P., and B. Kaina.** 2006. DNA damage-induced cell death by apoptosis. Trends Mol. Med. **12:**440–450.
55. **Schildgen, O., A. Muller, T. Allander, I. M. Mackay, S. Volz, B. Kupfer, and A. Simon.** 2008. Human bocavirus: passenger or pathogen in acute respiratory tract infections? Clin. Microbiol. Rev. **21:**291–304.
56. **Schmidt, M., S. Afione, and R. M. Kotin.** 2000. Adeno-associated virus type 2 Rep78 induces apoptosis through caspase activation independently of p53. J. Virol. **74:**9441–9450.
57. **Schwartz, D., B. Green, L. E. Carmichael, and C. R. Parrish.** 2002. The canine minute virus (minute virus of canines) is a distinct parvovirus that is most similar to bovine parvovirus. Virology **302:**219–223.
58. **Sol, N., J. Le Junter, I. Vassias, J. M. Freyssinier, A. Thomas, A. F. Prigent, B. B. Rudkin, S. Fichelson, and F. Morinet.** 1999. Possible interactions between the NS-1 protein and tumor necrosis factor alpha pathways in erythroid cell apoptosis induced by human parvovirus B19. J. Virol. **73:**8762–8770.

59. **Stracker, T. H., G. D. Cassell, P. Ward, Y. M. Loo, B. van Breukelen, S. D. Carrington-Lawrence, R. K. Hamatake, P. C. van der Vliet, S. K. Weller, T. Melendy, and M. D. Weitzman.** 2004. The Rep protein of adeno-associated virus type 2 interacts with single-stranded DNA-binding proteins that enhance viral replication. J. Virol. **78:**441–453.
60. **Sun, Y., A. Y. Chen, F. Cheng, W. Guan, F. B. Johnson, and J. Qiu.** 2009. Molecular characterization of infectious clones of the minute virus of canines reveals unique features of bocaviruses. J. Virol. **83:**3956–3967.
61. **Tauer, T. J., M. H. Schneiderman, J. K. Vishwanatha, and S. L. Rhode.** 1996. DNA double-strand break repair functions defend against parvovirus infection. J. Virol. **70:**6446–6449.
62. **Tennant, R. W., K. R. Layman, and R. E. Hand.** 1969. Effect of cell physiological state on infection by rat virus. J. Virol. **4:**872–878.
63. **Teodoro, J. G., D. W. Heilman, A. E. Parker, and M. R. Green.** 2004. The viral protein Apoptin associates with the anaphase-promoting complex to induce G2/M arrest and apoptosis in the absence of p53. Genes Dev. **18:** 1952–1957.
64. **Weitzman, M. D., C. T. Carson, R. A. Schwartz, and C. E. Lilley.** 2004. Interactions of viruses with the cellular DNA repair machinery. DNA Repair (Amsterdam) **3:**1165–1173.
65. **Winocour, E., M. F. Callaham, and E. Huberman.** 1988. Perturbation of the cell cycle by adeno-associated virus. Virology **167:**393–399.